Photochemistry and Photobiology, 2007, 83: 232–235

X-Ray Crystallographic Analysis of 9-*cis*-Rhodopsin, a Model Analogue Visual Pigment†

Hitoshi Nakamichi[1] and Tetsuji Okada*[1,2]

[1]Biological Information Research Center, National Institute of Advanced Industrial Science and Technology, 2-41-6 Aomi, Koto-ku, Tokyo 135-0064, Japan
[2]Core Research for Evolution Science and Technology (CREST), Japan Science and Technology Agency, Japan

Received 13 June 2006; accepted 26 July 2006; published online 31 July 2006; DOI: 10.1562/2006-13-RA-920

ABSTRACT

Recent progress in high-resolution structural study of rhodopsin has been enabled by a novel selective extraction procedure with rod photoreceptor cells. In this study, we applied the method for rapid and efficient preparation of a purified analogue pigment using bovine rod outer segment membranes with 9-*cis*-retinal. After complete bleaching of the membranes and subsequent regeneration with the exogenous retinal, 9-*cis*-rhodopsin is selectively extracted from the membranes using combination of zinc and heptylthioglucoside. The solubilized sample, even with a small amount of contaminating retinal oximes, is shown to be pure enough for three-dimensional crystallization. The X-ray diffraction from 9-*cis*-rhodopsin crystals was examined and the electron density map at 2.9 Å resolution in the chromophore region can be fitted well with the model of 9-*cis*-retinal Schiff base.

INTRODUCTION

Interaction between a cofactor and the surrounding polypeptide moiety is affected depending on the functional state of protein. Vice versa the physico-chemical properties of a cofactor can be a good probe for investigating molecular mechanism of the protein dynamics. In the case of visual pigments, the apoprotein moiety, opsin, is strictly constrained in a quiescent form in the dark, owing to intramolecular interactions with the chromophore, 11-*cis*-retinal. Rhodopsin, a scotopic photoreceptor in the rod cells, exhibits a visible absorption maximum at about 500 nm, which is a consequence of the specific retinal-protein interactions in the ground state. Upon absorption of a photon, the retinal isomerizes to its all-*trans* form (1–3), and the following thermal reaction gives rise to a series of photoreaction intermediate states having distinct spectroscopic properties (4,5). This photo-activation process of rhodopsin has been investigated with a variety of biophysical techniques.

11-*cis*-Retinal acts as an inverse-agonist, in terms of its negative effect on the light-independent constitutive activity of the opsin molecule (6). It has been generally assumed that chromophore–protein interaction changes during the photo-activation of rhodopsin would represent some common activation mechanism shared by the other members in the rhodopsin-like G protein-coupled receptor (GPCR) family (7). The strict intramolecular restraint that 11-*cis*-retinal provides to opsin might be outstanding among huge number of combinations between GPCRs and their ligand molecules: the activity of rhodopsin to catalyse GDP/GTP exchange on the α-subunit of G protein transducin is extremely lowered upon covalent binding of 11-*cis*-retinal to the side chain of Lys296 in the middle of transmembrane helix VII (7) and this mechanism provides the basis of low dark noise in the scotopic vision.

On the other hand, the chromophore binding pocket of rhodopsin has been also known to accommodate a variety of retinal isomers and analogues, with consequent changes in photobleaching behavior and activity (8–10). Therefore, detailed structural studies on such analogue pigments are expected to provide valuable information about the ligand-induced structural changes. High-resolution X-ray crystallographic analysis has become successful recently on bovine rhodopsin (11–13). Tetragonal crystals (11,13) appear from the sample obtained by a novel purification procedure, the highly selective solubilization of the rod outer segment (ROS) membranes (14). It provided rhodopsin sample of enough purity and concentration for three-dimensional crystallization (15). Because the method performs quite reproducibly, it was expected to be applicable to ROS membranes regenerated with an artificial retinal and enable crystallographic studies on analogue pigments of rhodopsin. Here we present a rapid and practical method for preparation and three-dimensional crystallization of the 9-*cis* analogue pigment (isorhodopsin) as a model system because 9-*cis*-retinal is known to bind to opsin efficiently (16). Also its medium resolution diffraction data are shown to be sufficient for discriminating the chromophore structure from closely resembling 11-*cis* isomer.

MATERIALS AND METHODS

Bovine ROS membranes were prepared by the procedure reported elsewhere (17). 9-*cis*-Retinal was either purchased from Sigma or obtained by HPLC (LC-10AT, Shimadzu) as described previously (18). Absorption spectra were obtained by Shimadzu UV-2450 spectrophotometer. Crystallization results were monitored by a microscope (Olympus) which was modified to pass only the > 650 nm light. The crystals were frozen in liquid nitrogen and the diffractions were

†This paper is part of the Proceedings of the 12th International Conference on Retinal Proteins held at Awaji Island, Hyogo, Japan on 4–8 June 2006.
*Corresponding author email: t-okada@aist.go.jp (Tetsuji Okada)

examined at BL41XU in SPring-8, Japan. The data were processed with HKL2000 (19) and map calculation and refinement were done with CNS (20).

RESULTS AND DISCUSSION

In general, crystallization of a complex between a cofactor/ligand and a protein might be possible either before or after preparing the crystal of a protein of interest. For visual rhodopsin from natural source, in which 11-*cis*-retinal is covalently bound to opsin via protonated Schiff base, simple soaking of an excess amount of exogenous retinal analogue does not result in chromophore exchange. Thus it is necessary first to bleach the ROS membrane completely in the presence of hydroxylamine. Then the bleached membranes exhibit only the absorption band of all-*trans*-retinal oximes around 365 nm and that of the protein, mostly from aromatic residues at 280 nm (Fig. 1a, broken curve).

The membranes containing opsin and all-*trans*-retinal oxime were subsequently washed with a buffer 25 m*M* MES/200 m*M* NaCl (pH 6.4) to reduce the concentration of hydroxylamine to less than 10 μ*M*. An excess molar amount of 9-*cis*-retinal was then added to the membrane suspension and the mixture was incubated at room temperature (22–24 °C) for 2 h (solid curve). The degree of regeneration was monitored by visible absorption spectroscopy using an aliquot from the mixture. After completion of the reaction, the excess retinal was converted to the oxime by adding 1 m*M* hydroxylamine (dotted curve). Finally, the membranes were washed again with distilled water to reduce the concentration of both NaCl and hydroxylamine to less than 2 m*M* and 10 μ*M*, respectively, in order not to interfere the subsequent solubilization process.

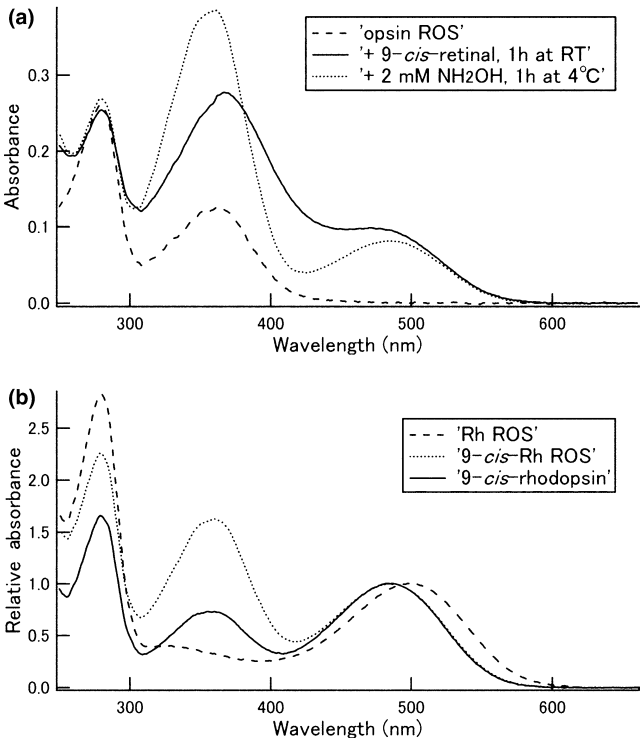

Figure 1. Absorption spectra obtained during the preparation of 9-*cis* rhodopsin. (a) membrane preparation. broken, starting opsin membranes; solid, regenerated membranes with 9-*cis*-retinal; dotted, after conversion of 9-*cis*-retinal to its oxime. b) selective extraction. broken, ROS membranes; dotted, 9-*cis*-rhodopsin membranes; solid, purified 9-*cis*-rhodopsin.

The membranes regenerated fully with 9-*cis*-retinal were then concentrated to about 7.0–8.5 mg mL^{-1} of isorhodopsin and mixed with a set of reagents that have been optimized for selective solubilization (14). The final concentrations of each component were: 5 mg mL^{-1} isorhodopsin, 1.1–1.3% heptylthioglucoside, 100 m*M* zinc acetate, 30 m*M* MES (pH 6.4). The optimal amount of the detergent can be estimated by visual inspection of the increase in the turbidity of the suspension and clear separation of the insoluble material by quick spin (2000 × ***g***, 1 min). Then, the mixture was suspended again and incubated further for 4–5 h at room temperature. Then the sample was centrifuged at 7740 × ***g*** for 3 minutes and the clear supernatant was collected. A typical absorption spectrum of the purified 9-*cis*-rhodopsin is shown in Fig. 1b (solid curve). The absorption maximum of 485 nm is blue-shifted by 15 nm from that of rhodopsin purified in the same manner or in the ROS membrane (broken curve). The absorption ratio A280/A485, a measure of pigment purity, is close to 1.6 which is the minimum value known for bovine rhodopsin (14,21).

The advantage of our selective extraction method is that only a limited amount of lipids is left associated with rhodopsin (14). This feature is clearly demonstrated by the fact that the amount of retinal oxime, which is expected to coexist with lipids, is remarkably smaller in the purified sample compared with the starting regenerated membranes. The absorption ratios A365/A485 for the curves dotted and solid in Fig. 1b are 1.6 and 0.7, respectively. As shown below, the small amount of oxime remaining in the purified sample does not significantly affect the three-dimensional crystallization process.

The purified 9-*cis*-rhodopsin was subjected to some trials for three-dimensional crystallization as previously described for native bovine rhodopsin (13). In brief, 100 μL of the sample solution was first mixed with a set of crystallization reagents to give the final concentrations as follows: 3.5 mg mL^{-1} isorhodopsin, 1.4–1.6% heptylthioglucoside, 70 m*M* zinc acetate, 20 m*M* MES (pH 6.4), 5 m*M* 2-mercaptoethanol, 0.85 *M* ammonium sulfate. 6–10 μL from the mixture was used for a hanging drop, which was equilibrated with 500 μL reservoir solution containing 25 m*M* MES (pH 5.9–6.0) and 2.8–3.1 *M* ammonium sulfate. The crystallization plates were inspected in the dark with a microscope having a cut-off filter of > 650 nm light to avoid photoreaction.

The picture of a 9-*cis*-rhodopsin crystal is shown in Fig. 2b. Its rod-shaped morphology is similar to that of rhodopsin (Fig. 2a) and the longest dimension occasionally reaches more than 1 mm. By microspectrophotometry, we have also confirmed the absorption spectrum of the crystal of 9-*cis*-rhodopsin to be blue-shifted from that of rhodopsin (data not shown).

Crystals are frozen in liquid nitrogen with 15% trehalose as the cryoprotectant. The X-ray diffraction images were collected with a synchrotron X-ray beam on a Mar165 CCD detector in BL41XU at SPring-8 (Harima, Japan) with the beam wavelength of 1.0000 Å. The temperature of the nitrogen gas at the position of the crystal was kept at 90 K during data collection. The oscillation images were processed with

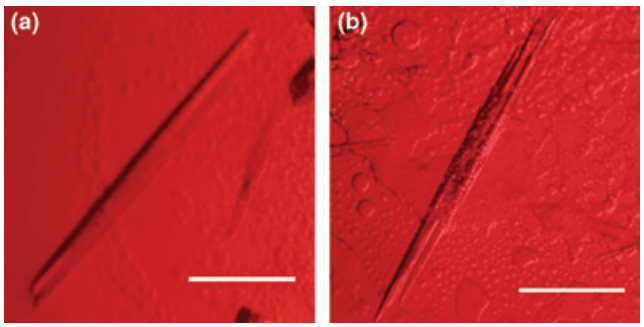

Figure 2. Photographs of the three-dimensional crystals of a) 11-*cis* and b) 9-*cis*-rhodopsin. Scale bars 0.3 mm.

Table 1. X-ray diffraction data statistics.

	Data 1	Data 2
Beamline	BL41XU, SP-8	BL41XU, SP-8
Resolution, Å	50–2.9	50–2.9
Unit cell (a = b, c), Å*	95.65, 151.4	95.96, 150.8
Twin fraction	0.102	0.000
Mosaicity °	0.86	1.07
Total observations	98,215	97,139
Unique observations	28,034	27,964
R_{merge}, % (outer shell)	14.8 (76.9)	13.9 (77.8)
Completeness, % (outer shell)	92.5 (54.3)	91.8 (53.2)
I/σ (I) (outer shell)	8.04 (1.04)	8.27 (1.06)
Wilson *B* factor, Å^2	50.0	56.8

*The space group is $P4_1$. $R_{merge} = \Sigma_{hkl} \Sigma_i \mid I_i(hkl) - < I(hkl) > \mid / \Sigma_{hkl} \Sigma_i I_i(hkl)$.

HKL2000. In Table 1, the statistics of the two data sets to 2.9 Å resolution are summarized. Importantly, one of them is completely free of merohedral twinning which has been a problem during the analyses of rhodopsin structure in a tetragonal space group (11,13,15).

For structure refinement of 9-*cis*-rhodopsin, the previously determined rhodopsin model at 2.2 Å resolution was used as a starting geometry. After rigid body refinement, the model was subjected to simulated-annealing and conjugate gradient energy minimization with CNS. The initial parameters for the retinal were the same as those used in the previous refinement of rhodopsin except the dihedral angles around the C9 = C10 and C11 = C12 double bonds. As shown in Fig. 3, the omit map calculated by removing the chromophore binding site could be fitted better with the 9-*cis* form than with the 11-*cis* form of retinal. Thus, we can clearly discriminate these two isomeric forms in the binding pocket of rhodopsin despite the fact that the current resolution for 9-*cis*-rhodopsin is lower than that obtained for rhodopsin. Taking into account the considerably limited number of current crystallization trials for 9-*cis*-rhodopsin and our routine observation that the diffraction limit of rhodopsin crystals still varies from 3.5 to 2.0 Å resolution, it appears possible to obtain even higher quality data for some of the other analogue pigments prepared by the procedure described in this study.

Because the current model of isorhodopsin indicates that the residues surrounding retinal are not much affected by the exchange of the isomeric form from 11-*cis* to 9-*cis*, it is difficult at this stage to give a conclusive explanation for the differences between rhodopsin and isorhodopsin with respect to the speed of regeneration with opsin, the stability of the regenerated pigment and the energetic state (22). Another known interesting difference between rhodopsin and 9-*cis*-rhodopsin is the lower quantum efficiency of the latter (23), which might be partly explained by the intrinsic properties of the corresponding retinal protonated Schiff bases (24). In a recently proposed crystallographic model of the primary intermediate bathorhodopsin (3), the C9 methyl group appears to work as a critical structural point. Thus it is possible that the proximity of the isomerizing C9 = C10 double bond to this group would be less favorable for the photoreaction. Further improvement of the diffraction data quality will provide a more detailed picture with regard to the mechanism of high quantum efficiency of rhodopsin.

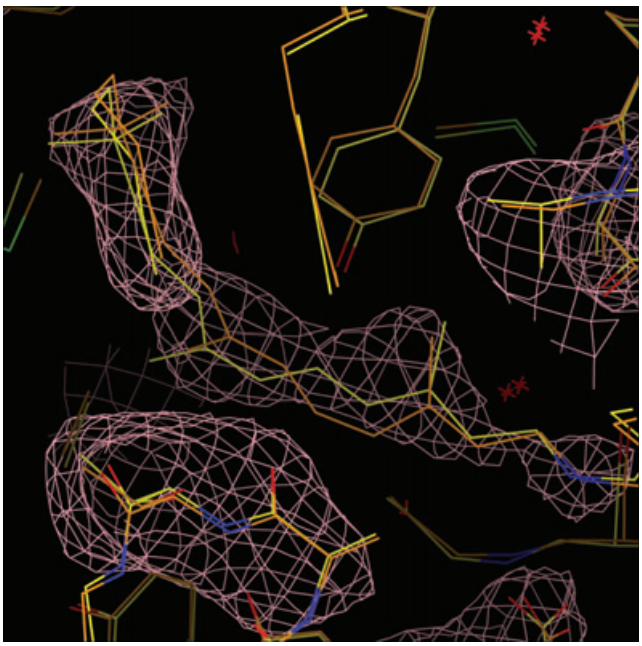

Figure 3. Electron density of 9-*cis*-retinal chromophore. A simulated-annealed omit map was calculated using the structure factor amplitudes from a 9-*cis*-rhodopsin crystal and phases from the model excluding retinal and nearby region within 4.5 angstroms. 9-*cis* and 11-*cis* retinals along with the nearby protein carbons are shown in yellow and orange, respectively. Oxygen and nitrogen atoms are colored red and blue, respectively.

In summary, we have shown that an analogue visual pigment containing 9-*cis*-retinal can be crystallized and analyzed at moderate resolution. The present study should be a good starting point for the structural analyses of more challenging artificial pigments whose properties significantly differ from those of rhodopsin.

Acknowledgements—This work has been supported in part by grants from the Japanese Ministry of Education, Culture, Sports, Science and Technology, and by NEDO. We are grateful to H. Sakai and M. Kawamoto for excellent support at BL41XU of SPring-8.

REFERENCES

1. Schoenlein, R. W., L. A. Peteanu, R. A. Mathies and C. V. Shank (1991) The first step in vision: Femtosecond isomerization of rhodopsin. *Science* **254**, 412–415.

2. Kandori, H., Y. Shichida and T. Yoshizawa (2001) Photoisomerization in rhodopsin. *Biochemistry (Moscow)* **66**, 1197–1209.
3. Nakamichi, H. and T. Okada (2006) Crystallographic analysis of primary visual photochemistry. *Angew. Chem. Int. Ed.* **45**, 4270–4273.
4. Vogel, R. and F. Siebert (2003) Fourier transform IR spectroscopy study for new insights into molecular properties and activation mechanisms of visual pigment rhodopsin. *Biopolymers* **72**, 133–148.
5. Lewis, J. W. and D. S. Kliger (1992) Photointermediates of visual pigments. *J. Bioenerg. Biomembr.* **24**, 201–210.
6. Surya, A., J. M. Stadel and B. E. Knox (1998) Evidence for multiple, biochemically distinguishable states in the G protein-coupled receptor, rhodopsin. *Trends Pharmacol. Sci.* **19**, 243–247.
7. Okada, T., O. Ernst, K. Palczewski and K. P. Hofmann (2001) Activation of rhodopsin: New insights from structural and biochemical studies. *Trends Biochem. Sci.* **26**, 318–324.
8. Corson, D. W. and R. K. Crouch (1996) Physiological activity of retinoids in natural and artificial visual pigments. *Photochem. Photobiol.* **63**, 595–600.
9. Nakanishi, K., H. Zhang, K. A. Lerro, S. Takekuma, T. Yamamoto, T. H. Lien, L. Sastry, D. J. Baek, C. Moquin-Pattey, M. F. Boehm, F. Derguini and M. A. Gawinowics (1995) Photoaffinity labeling of rhodopsin and bacteriorhodopsin. *Biophys. Chem.* **56**, 13–22.
10. Ottolenghi, M. and M. Sheves (1989) Synthetic retinals as probes for the binding site and photoreactions in rhodopsins. *J. Membr. Biol.* **112**, 193–212.
11. Palczewski, K., T. Kumasaka, T. Hori, C. A. Behnke, H. Motoshima, B. A. Fox, I. LeTrong, D. C. Teller, T. Okada, R. E. Stenkamp, M. Yamamoto and M. Miyano (2000) Crystal structure of rhodopsin: A G protein-coupled receptor. *Science* **289**, 739–745.
12. Li, J., P. C. Edwards, M. Burghammer, C. Villa and G. F. Schertler (2004) Structure of bovine rhodopsin in a trigonal crystal form. *J. Mol. Biol.* **343**, 1409–1438.
13. Okada, T., M. Sugihara, A.-N. Bondar, M. Elstner, P. Entel and V. Buss (2004) The retinal conformation and its environment in the light of new 2.2 crystal structure. *J. Mol. Biol.* **342**, 571–583.
14. Okada, T., K. Takeda and T. Kouyama (1998) Highly selective separation of rhodopsin from bovine rod outer segment membranes using combination of divalent cation and alkyl(thio)glucoside, *Photochem. Photobiol.* **67**, 495–499.
15. Okada, T., I. LeTrong, B. A. Fox, C. A. Behnke, R. E. Stenkamp and K. Palczewski (2000) X-ray diffraction analysis of three-dimensional crystals of bovine rhodopsin obtained from mixed micelles. *J. Struct. Biol.* **130**, 73–80.
16. Hubbard, R. and G. Wald (1952) *Cis-trans* isomers of vitamin A and retinene in the rhodopsin system. *J. Gen. Physiol.* **36**, 269–315.
17. Okada, T., R. Tsujimoto, M. Muraoka and C. Funamoto (2005) Methods and results in the x-ray crystallography of bovine rhodopsin. In *G Protein-Coupled Receptors: Structure, Function and Ligand Screening* (Edited by T. Haga and S. Takeda), CRC Press, Boca Raton, FL.
18. Shichida, Y., H. Kandori, T. Okada, T. Yoshizawa, N. Nakashima and K. Yoshihara (1991) Differences in the photobleaching process between 7-*cis*- and 11-*cis*-rhodopsins: A unique interaction change between the chromophore and the protein during the Lumi-Meta I transition. *Biochemistry* **30**, 5918–5926.
19. Otwinowski, Z. and W. Minor (1997) Processing of X-ray diffraction data collected in oscillation mode. *Methods Enzymol.* **276**, 307–326.
20. Brünger, A. T., P. D. Adams, G. M. Clore, W. L. DeLano, P. Gros, R. W. Grosse-Kunstleve, J. S. Jiang, J. Kuszewski, M. Nilges, N. S. Pannu, R. J. Read, L. M. Rice, T. Simonson and G. L. Warren (1998) Crystallography & NMR system: A New software suite for macromolecular structure determination. *Acta Crystallogr.* **54**, 905–921.
21. Lin, S. W. and T. P. Sakmar (1996) Specific tryptophan UV-absorbance changes are probes of the transition of rhodopsin to its active state. *Biochemistry* **35**, 11149–11159.
22. Cooper, A. (1979) Energetics of rhodopsin and isorhodopsin. *FEBS Lett.* **100**, 382–384.
23. Birge, R. R., C. M. Einterz, H. M. Knapp and L. P. Murray (1988) The nature of the primary photochemical events in rhodopsin and isorhodopsin. *Biophys. J.* **53**, 367–385.
24. Freedman, K. A. and R. S. Becker (1986) Comparative investigation of the photoisomerization of the protonated and unprotonated n-butylamine Schiff base of 9-*cis*-, 11-*cis*-, 13-*cis*, and all-trans-retinals. *J Am. Chem. Soc.* **108**, 1245–1251.